BRAIN
ORIGINAL ARTICLE

Altered T-cell reactivity in the early stages of Alzheimer's disease

Chiara Rickenbach,[1] Anna Mallone,[2] Lars Häusle,[1,2] Larissa Frei,[1] Sarina Seiter,[1] Colin Sparano,[3] Tunahan Kirabali,[1] Kaj Blennow,[4,5,6,7] Henrik Zetterberg,[4,5,8,9,10,11] Maria Teresa Ferretti,[12] Luka Kulic,[13] Christoph Hock,[1,14,15] Roger M. Nitsch,[1,15] Valerie Treyer,[1,14,16,†] Anton Gietl[1,14,17,†] and Christoph Gericke[1,†]

[†]These authors contributed equally to this work.

The adaptive immune system and neurodegenerative Alzheimer's disease (AD) are intertwined in multiple ways. Recent studies have reported alterations of the adaptive immune system in early AD stages, such as preclinical AD and mild cognitive impairment (MCI) due to AD. However, the identity of specific antigenic targets and whether the respective response is beneficial or detrimental during disease progression are still open questions.

Herein, we describe cross-sectional analyses of blood and CSF from three different study populations covering early AD stages. We employed high-dimensional mass cytometry, single-cell RNA-sequencing, *ex vivo* T-cell secretome analysis, and antigen presentation assays to achieve a comprehensive characterization of adaptive immune cell populations.

Our results show that subjects at the stage of asymptomatic, preclinical AD can mount a $CD4^+$ T helper cell response towards amyloid-β peptide and display an early enrichment of $CD8^+$ T effector memory cells re-expressing CD45RA (TEMRA cells) in CSF, combined with a less immunosuppressive gene signature of peripheral regulatory T cells. Conversely, in MCI we observed increased frequencies of $CD8^+$ TEMRA/effector cells in the periphery characterized by a pro-inflammatory gene expression profile, and generally decreased antigen responsiveness.

Our results demonstrate the complexity of adaptive immune changes in early AD and suggest that it may be beneficial to promote specific $CD4^+$ T-cell responses in the preclinical stage, while in MCI it may be important to therapeutically target $CD8^+$ T-cell responses if these prove to be harmful.

1 Institute for Regenerative Medicine—IREM, University of Zurich, 8952 Schlieren, Switzerland
2 Institute of Microbiology, ETH Zurich, 8049 Zurich, Switzerland
3 Institute of Experimental Immunology, University of Zurich, 8057 Zurich, Switzerland
4 Department of Psychiatry and Neurochemistry, Institute of Neuroscience and Physiology, Sahlgrenska Academy, University of Gothenburg, S-43180 Mölndal, Sweden
5 Clinical Neurochemistry Laboratory, Sahlgrenska University Hospital, S-43180 Mölndal, Sweden
6 Paris Brain Institute, ICM, Pitié-Salpêtrière Hospital, Sorbonne University, 75013 Paris, France
7 Neurodegenerative Disorder Research Center, Division of Life Sciences and Medicine, and Department of Neurology, Institute on Aging and Brain Disorders, University of Science and Technology of China and First Affiliated Hospital of USTC, 230026 Hefei, China
8 Department of Neurodegenerative Disease, UCL Institute of Neurology, Queen Square, London WC1N 3BG, UK

Received August 21, 2024. Revised March 14, 2025. Accepted April 10, 2025. Advance access publication May 5, 2025

9 UK Dementia Research Institute at UCL, London WC1N 3BG, UK
10 Hong Kong Center for Neurodegenerative Diseases, Clear Water Bay, Hong Kong, China
11 Wisconsin Alzheimer's Disease Research Center, University of Wisconsin School of Medicine and Public Health, University of Wisconsin-Madison, Madison, WI 53792, USA
12 Center for Alzheimer Research, Karolinska Institute, S-17177 Stockholm, Sweden
13 Roche Pharma Research and Early Development, Roche, 4070 Basel, Switzerland
14 Center for Prevention and Dementia Therapy, University of Zurich, 8952 Schlieren, Switzerland
15 Neurimmune AG, 8952 Schlieren, Switzerland
16 Department of Nuclear Medicine, University Hospital Zurich, 8091 Zurich, Switzerland
17 Psychiatric University Hospital Zurich (PUK), 8008 Zurich, Switzerland

Correspondence to: Christoph Gericke
Institute for Regenerative Medicine—IREM, University of Zurich
Campus Schlieren, Wagistrasse 12, 8952 Schlieren, Zurich, Switzerland
E-mail: christoph.gericke@irem.uzh.ch

Keywords: Alzheimer's disease (AD); AD biomarkers; CyTOF; scRNA-seq; T cells; antigen specificity

Introduction

Alzheimer's disease (AD) is a neurodegenerative disease affecting over 50 million people worldwide.[1] Hallmarks of AD pathology are aggregation and deposition of misfolded amyloid-β peptide (Aβ) into Aβ plaques, neurofibrillary tangles of hyperphosphorylated tau, and neurodegeneration.[2] After a long asymptomatic preclinical phase with Aβ accumulation followed by tau pathology, AD can progress along a continuum to mild cognitive impairment (MCI) and dementia.[3-7] Biomarkers for AD, including cerebral Aβ and tau aggregates measured by PET scans, along with elevated levels of phosphorylated tau species (p-tau) in CSF or plasma, can predict the probability of a clinical transition from cognitively healthy individuals to MCI and dementia.[8-10] Importantly, preclinical AD refers to cognitively normal individuals with increased risk, rather than a certainty of progression to MCI or AD, as many biomarker-positive, cognitively unimpaired individuals remain stable for extended periods while others do progress.[11] As particularly the preclinical phase of AD is not well understood, its in-depth characterization would allow improving biomarkers and potentially preventive therapeutic strategies before the onset of symptoms.

In recent years, the role of adaptive immunity in AD has been increasingly recognized. Both clinical and genetic data suggest an involvement of inflammation-related pathways in AD pathogenesis and progression.[12,13] Multiple studies have identified increased T-cell infiltration in AD brains,[14-16] sparking the question of whether the underlying responses might be beneficial or detrimental during disease progression. For the $CD8^+$ subtype of T cells, T effector memory cells re-expressing CD45RA (TEMRA) were shown to be increased in peripheral blood and CSF of AD patients.[14] Interestingly, immunophenotyping studies focusing on earlier stages of AD revealed that $CD8^+$ TEMRA cells are altered even before the conversion to AD dementia[17] as early as in preclinical AD.[18] While lymphocyte infiltration in AD brains appears to be a targeted process, the antigenic target remains unknown.[19] Some studies investigated the T-cell antigen specificity in AD and reported reactivity of $CD4^+$ T cells towards Aβ-derived epitopes in a human leucocyte antigen (HLA) class II-dependent manner.[20-22] These results were no surprise as earlier studies observed that immunization with Aβ peptide resulted in less AD pathology in mouse models of β-amyloidosis.[23] The subsequent first active immunization strategy for AD was AN-1792, mainly consisting of synthetic full-length $Aβ_{1-42}$ peptide. Clinical trials were suspended due to cases of meningoencephalitis.[24] Nevertheless, T-cell recruitment to the CNS occurred, and some responders mounted antibody responses against the amino-terminus (N-terminus) of Aβ.[25] Further discoveries of human autoantibodies directed against aggregated Aβ support the concept of successful priming of the adaptive immune system in AD.[26-28]

To investigate the onset, targets and nature of AD-associated T-cell responses, we performed an in-depth cross-sectional immunophenotyping of three study populations covering the early stages of AD. We included cognitively healthy subjects with early evidence of cerebral β-amyloidosis (referred to as preclinical AD) and subjects with MCI due to AD (also referred to as prodromal AD). We provide a detailed analysis of immune cell populations in peripheral blood and CSF by combining mass cytometry by time-of-flight (CyTOF) and single-cell RNA sequencing (scRNA-seq). Additionally, we performed a functional analysis of the T-cell secretome and antigen presentation assays. We report that $CD4^+$ T cells in preclinical AD display a type 2 T-helper profile and reactivity against carboxyl-terminal (C-terminal) and mid-sequence peptides derived from linear $Aβ_{1-42}$. In contrast, we observe an increased frequency and a more pro-inflammatory gene expression of $CD8^+$ TEMRA/effector cells in MCI subjects. Our analysis suggests a potentially beneficial role for activated $CD4^+$ T helper cells in preclinical AD and a potentially harmful involvement of $CD8^+$ T cells when the pathology becomes clinically symptomatic.

Materials and methods

Study design

The goal of this study was to investigate the immunophenotype and function of $CD4^+$ and $CD8^+$ T cells in individuals categorized as potential preclinical cases of AD and in participants diagnosed with MCI (according to consensus criteria[29]). As material we used peripheral blood mononuclear cells (PBMCs) or CSF-derived cells, blood plasma and serum from healthy control subjects (HCS) and participants with MCI. All participants were part of an ongoing monocentric and prospective longitudinal cohort study with extensive multimodal imaging, fluid biomarker analysis, as well as clinical and cognitive assessments ('ID-Cog' study[18,30] and Tables 1–3).

Table 1 Demographics and clinical characteristics of study population 1

	Total	HCS−	HCS+	Group differences
Subjects	9	5	4	
Age, mean ± SD [range]	65.6 ± 9.0 [50–78]	65.4 ± 10.7 [50–78]	65.8 ± 7.8 [56–75]	$t = 0.06$, $P = 0.9564$
Sex, male/female	7/2	4/1	3/1	$\chi^2 = 0.03$, $P = 0.8577$
Years of education, mean ± SD	16.1 ± 2.7	16.6 ± 2.3	15.5 ± 3.3	$t = 0.56$, $P = 0.5966$
APOE ε4 carriers	55.6%	60.0%	50.0%	$\chi^2 = 0.09$, $P = 0.7642$
CSF $A\beta_{40}$, median [IQR] in pg/ml	7984.5 [3412.7]	7262.5 [3174.5]	9426.6 [3590.2]	Mann–Whitney $U = 4$, $P = 0.1905$
CSF $A\beta_{42}$, median [IQR] in pg/ml	626.9 [155.7]	626.9 [222.1]	600.6 [248.3]	Mann–Whitney $U = 8$, $P = 0.7302$
CSF $A\beta_{42}$/ $A\beta_{40}$, median [IQR]	0.079 [0.020]	0.086 [0.007]	0.065 [0.004]	Mann–Whitney $U = 0$, $P = 0.0159$
CSF total tau, median [IQR] in pg/ml	160.3 [74.3]	118.0 [83.0]	176.3 [58.7]	Mann–Whitney $U = 5$, $P = 0.2857$

Study population 1 includes cognitively healthy control subjects (HCS) grouped according to CSF amyloid-β $(A\beta)_{42/40}$ ratio into brain Aβ-negative (HCS− = high CSF $A\beta_{42/40}$ ratio = elderly and unaffected) and Aβ-positive (HCS+ = low CSF $A\beta_{42/40}$ ratio = potentially preclinical Alzhiemer's disease). Normally distributed variables are summarized as mean with standard deviation (SD). Non-normally distributed variables are summarized as median with interquartile range (IQR). Group differences were calculated using parametric unpaired *t*-test with Welch's correction (for parameters 'Age' and 'Years of education') or non-parametric Mann–Whitney test (for CSF biomarkers). The *P*-values for categorical variables such as 'Sex' and '*APOE* ε4 carriers' were calculated using Chi-square test for independence.

For the analyses, three subpopulations of study participants were selected from the overall study population at baseline to conduct three cross-sectional analyses (Fig. 1). Due to the exploratory nature of these three cross-sectional analyses, no *a priori* power analysis was conducted to estimate sample sizes. Where possible, a balanced ratio of female and male study participants was aimed for in the study populations. We performed an in-depth analysis of the immunophenotype using CyTOF and scRNA-seq for study populations 1 and 2, as well as a functional analysis of the T-cell secretome and antigen presentation assays for study population 3.

Study participants

Study population 1 included nine study participants representing a subgroup that consented to lumbar puncture for CSF collection. Study population 1 was categorized based on the ratio of CSF AD biomarkers $A\beta_{42}$ and $A\beta_{40}$ into brain Aβ-negative (HCS− = high CSF $A\beta_{42/40}$ ratio = elderly and unaffected) and Aβ-positive (HCS+ = low CSF $A\beta_{42/40}$ ratio = potentially preclinical AD).

Study population 2 included 30 participants and study population 3 included 44 participants. Both were assessed for cerebral Aβ load measured via PET imaging using ^{18}F-flutemetamol (FMM) tracer. The median time difference between PBMC sampling and PET imaging was 19 days. To standardize quantitative Aβ imaging measurements, the 'Centiloid' approach was used.[31] The Centiloid cut-off for Aβ positivity was set at FMM Centiloid >12, which has been shown to mark the transition from absence of pathology to subtle pathology.[32] Study participants were grouped based on Aβ PET into Aβ-negative and Aβ-positive HCS (HCS− and HCS+) and Aβ-positive MCI (MCI+). Study populations 2 and 3 additionally underwent plasma AD biomarker analysis for $A\beta_{42}$ and $A\beta_{40}$, as well as phospho-tau 217 (p-tau217), neurofilament light (NfL) and glial fibrillary acidic protein (GFAP). Subjects with current/recent tumours, Hashimoto's disease or increased serum levels of C-reactive protein (CRP) were excluded.

Ethics declaration

The participants included in the analyses participated in in-house cohort studies conducted by the 'Center for Prevention and Dementia Therapy' at the Institute for Regenerative Medicine at the University of Zurich, Switzerland. All study participants gave written informed consent. The cohort studies including the here shown assessments were approved by the local ethics committee (Kantonale Ethikkommission, Zurich, Switzerland) and conducted in accordance with their guidelines and the Declaration of Helsinki.[33]

APOE genotyping

APOE genotyping was performed using a restriction isotyping protocol[34] or Sanger Sequencing (Microsynth AG).

PET imaging and image analysis

Standard reconstructed PET/MRI ^{18}F-FMM-PET images were averaged over the time window between 85–105 min post injection. Images were acquired on a Signa PET/MRI (GE Healthcare). Participants received a maximum of 140 MBq of tracer. Images were processed with PMOD 4.0 NeuroTool (PMOD Technologies, Zurich, Switzerland) according to standard Centiloid methods.[31]

MRI and image analysis

Hippocampus parcellation was performed using FreeSurfer (v7.1.1, CentOS8) on FSPGR 3D T_1-weighted images (0.5 mm isotropic voxel size, axial slice orientation, repetition time/echo time/inversion time = 11/5.2/600 ms, flip angle = 8°). Parcellations were visually inspected for accuracy, with manual corrections applied as needed. Hippocampal volumes were adjusted for total intracranial volume (ICV). Values were previously reported for the whole cohort.[30]

Neuropsychological testing

Details of the neuropsychological testing within the cohort study were published previously.[18,30,35] For this analysis, we used Mini-Mental State Examination (MMSE) assessment for global estimate of cognitive functions.

Serology for anti-viral antibody titres

Antibody titres were analysed in serum samples via ELISA or indirect immunofluorescence at the Institute of Medical Virology, University of Zurich. Antibody titres against Cytomegalovirus (CMV) (IgG and IgM), Epstein–Barr virus (EBV) [IgG and IgM against viral capsid antigen (VCA) and IgG against Epstein–Barr nuclear antigen (EBNA)], Herpes simplex virus (HSV) 1 and 2 (IgG and IgM) and Varicella-Zoster Virus (VZV) (IgG and IgM) were measured. Quantitative results were obtained for the following antibody titres: VZV IgG (in mIU/ml, threshold for positive test >100), CMV IgG (in

Table 2 Demographics and clinical characteristics of study population 2

	Total	HCS−	HCS+	MCI+	Group differences
Subjects	30	10	10	10	
Age, mean ± SD [range]	72.1 ± 6.5 [59–85]	69.6 ± 4.3 [61–77]	69.5 ± 6.9 [59–80]	77.3 ± 4.9 [69–85]	$F(2,27) = 6.617$, $P = 0.0046$
Sex, male/female	15/15	5/5	7/3	3/7	$P = 0.2623$
Years of education, mean ± SD	14.8 ± 3.1	16.0 ± 3.2	15.8 ± 2.9	12.7 ± 1.8	$F(2,27) = 4.583$, $P = 0.0193$
MMSE, mean ± SD	28.5 ± 1.9	29.7 ± 0.5	28.8 ± 1.8	27.0 ± 1.9	$F(2,27) = 7.767$, $P = 0.0022$
APOE ε4 carriers	26.7%	10.0%	30.0%	40.0%	$P = 0.4499$
APOE ε2 carriers	13.3%	10.0%	10.0%	20.0%	$P > 0.9999$
FMM Centiloid, median [IQR]	47.8 [75.9]	−2.2 [2.1]	47.8 [10.0]	84.6 [38.2]	$H(2) = 23.910$ $P < 0.0001$
Plasma $A\beta_{40}$, median [IQR] in pg/ml	110.5 [31.9]	115.5 [34.7]	107.0 [19.7]	109.0 [43.7]	$H(2) = 0.420$ $P = 0.8105$
Plasma $A\beta_{42}$, median [IQR] in pg/ml	5.8 [2.7]	7.6 [1.6]	5.5 [1.2]	5.3 [1.4]	$H(2) = 5.933$ $P = 0.0515$
Plasma $A\beta_{42}$/ $A\beta_{40}$, median [IQR]	0.056 [0.016]	0.068 [0.011]	0.051 [0.008]	0.055 [0.010]	$H(2) = 6.745$ $P = 0.0343$
Plasma NfL, median [IQR] in pg/ml	27.0 [14.2]	22.2 [9.5]	27.1 [14.8]	31.2 [5.9]	$H(2) = 5.258$ $P = 0.0722$
Plasma GFAP, median [IQR] in pg/ml	144.0 [91.0]	126.0 [45.5]	122.5 [75.0]	198.5 [102.5]	$H(2) = 6.072$ $P = 0.0480$
Plasma p-tau217, median [IQR] in pg/ml	2.5 [2.2]	1.1 [1.2]	2.5 [1.4]	3.6 [2.2]	$H(2) = 10.590$ $P = 0.0050$

Study population 2 includes cognitively healthy control subjects (HCS) and individuals with mild cognitive impairment (MCI) grouped based on amyloid-β (Aβ) PET imaging into HCS −, HCS+ and MCI+. The proportion of individuals with at least one copy of the *APOE* ε4 allele, which is linked to higher Alzheimer's disease risk, were higher in Aβ-positive groups compared to Aβ-negative groups (not significant, ns), with one case of homozygous *APOE* ε4 genotype in HCS+. Normally distributed variables are summarized as mean with standard deviation (SD). Non-normally distributed variables are summarized as median with interquartile range (IQR). Group differences were calculated using parametric one-way ANOVA with Bonferroni's multiple comparison correction (for parameters 'Age', 'Years of education' and 'MMSE') or non-parametric Kruskal–Wallis test with false discovery rate (FDR) method of Benjamini and Hochberg (for parameters 'FMM Centiloid' and plasma biomarkers). The *P*-values for categorical variables such as 'Sex', '*APOE* ε4 carriers' and '*APOE* ε2 carriers' were calculated using Fisher's exact test. FMM = ^{18}F-flutemetamol; MMSE = Mini-Mental State Examination; NfL = neurofilament light; p-tau = phosphorylated tau.

AE/ml, threshold ≥6), HSV-1 IgG (in 'Signal divided by cut-off': S/CO, threshold >1) and HSV-2 IgG (in S/CO, threshold >1). All other titres were analysed qualitatively (positive/negative).

Fluid AD biomarkers

Blood of study participants was collected in ethylenediaminetetraacetic acid (EDTA) tubes (Vacutainer EDTA Tubes, BD), inverted 10 times and centrifuged at 1620*g* for 12 min at 6°C. Plasma supernatant was aliquoted and stored at −80°C. CSF samples were centrifuged within 30 min after lumbar puncture at 350*g* for 10 min to separate CSF cells from supernatant. CSF supernatant was aliquoted and frozen at −80°C. For biomarker analysis of study population 1, quantifications were performed by Quanterix corporation on a Simoa HD-X instrument using Simoa Human Neurology 3-plex A (N3PA) immunoassays for measuring CSF $A\beta_{42}$, $A\beta_{40}$ and total tau. Biomarker analysis for study populations 2 and 3 was performed in the laboratories of Prof. H. Zetterberg and Prof. K. Blennow (Sahlgrenska University Hospital, Mölndal, Sweden). In brief, quantifications of plasma markers $A\beta_{42}$, $A\beta_{40}$, NfL and GFAP were performed with a customized Neurology 4-plex A platform (Quanterix), plasma p-tau217 was measured with an in-house assay of University of Gothenburg. Fluid biomarker levels below the limit of quantitation (LOQ) were set at LOQ/2 according to standard approaches for left-censored LOQ data.[36]

Single-cell analysis techniques

A detailed overview of all single-cell analysis methods used in this study, including CyTOF, scRNA-seq and secretome and antigen presentation assays measured by spectral flow cytometry, is provided in the Supplementary material.

Statistical analysis

Statistical analysis was performed in RStudio using *rstatix* and *stats* packages.[37] Differences between two groups were tested with non-parametric, two-tailed, unpaired Wilcoxon rank sum test (Mann–Whitney U-test) for non-normally distributed variables. Differences between multiple groups containing non-normally distributed variables were tested with non-parametric Kruskal–Wallis test with correction for multiple comparisons using the Benjamini-Hochberg false discovery rate (FDR) approach. Correlations were calculated with Pearson's correlation ($\alpha = 0.05$, confidence interval 95%, two-tailed) and non-parametric Spearman's correlation ($\alpha = 0.05$, confidence interval 95%, two-tailed). Effects of age, sex and virus titres were estimated using linear regression models, and analysis was performed on the basis of corresponding residuals. Due to small cohort size, an FDR < 10% has been applied. Where possible, violin plots have been used to display numerical data. Horizontal lines represent the median calculated based on the density estimate.

Results

CyTOF immunophenotyping reveals elevated peripheral CD8$^+$ TEMRA/effector cells in early AD

To determine the immunophenotypes of individuals in the early AD continuum, we characterized adaptive immune cells in three study populations, all derived as a subset from a prospective cohort study (Fig. 1). First, we analysed CSF immune cells from individuals in study population 1 ($n = 9$), which included cognitively healthy control subjects (HCS) grouped according to CSF $A\beta_{42/40}$ ratio into brain Aβ-negative (HCS−) and Aβ-positive (HCS+ = potentially

Table 3 Demographics and clinical characteristics of study population 3

	Total	HCS−	HCS+	MCI+	Group differences
Subjects	44	15	14	15	
Age, mean ± SD [range]	70.6 ± 7.7 [53–89]	67.0 ± 6.8 [54–77]	69.3 ± 6.5 [59–79]	75.3 ± 7.5 [53–85]	$F(2,41) = 5.747$, $P = 0.0063$
Sex, male/female	22/22	4/11	12/2	6/9	$P = 0.0039$
Years of education, mean ± SD	15.0 ± 2.9	14.8 ± 3.0	16.1 ± 2.2	14.1 ± 3.1	$F(2,41) = 2.026$, $P = 0.1448$
MMSE, mean ± SD	28.3 ± 1.7	29.5 ± 0.8	27.9 ± 1.5	27.5 ± 1.8	$F(2,41) = 8.340$, $P = 0.0009$
APOE ε4 carriers	29.5%	6.7%	50.0%	33.3%	$P = 0.0327$
APOE ε2 carriers	18.2%	20%	21.4%	13.3%	$P = 0.8937$
FMM Centiloid, median [IQR]	22.0 [52.7]	−2.4 [3.3]	26.4 [26.7]	71.4 [59.4]	$H(2) = 32.430$ $P < 0.0001$
Plasma $A\beta_{40}$, median [IQR] in pg/ml	114.0 [35.1]	114.0 [23.5]	114.5 [33.4]	102.0 [36.3]	$H(2) = 0.717$ $P = 0.6987$
Plasma $A\beta_{42}$, median [IQR] in pg/ml	7.0 [2.6]	7.5 [1.3]	6.0 [2.7]	5.7 [2.7]	$H(2) = 5.299$ $P = 0.0707$
Plasma $A\beta_{42}$/ $A\beta_{40}$, median [IQR]	0.061 [0.018]	0.069 [0.012]	0.059 [0.019]	0.059 [0.009]	$H(2) = 4.988$ $P = 0.0826$
Plasma NfL, median [IQR] in pg/ml	21.6 [15.5]	19.5 [9.4]	18.4 [6.7]	30.1 [10.3]	$H(2) = 7.352$ $P = 0.0253$
Plasma GFAP, median [IQR] in pg/ml	117.5 [87.3]	108.0 [66.0]	102.2 [37.4]	195.0 [109.0]	$H(2) = 9.515$ $P = 0.0086$
Plasma p-tau217, median [IQR] in pg/ml	1.7 [2.3]	0.6 [1.3]	1.4 [1.6]	3.0 [2.3]	$H(2) = 11.470$ $P = 0.0032$

Study population 3 includes cognitively healthy control subjects (HCS) and individuals with mild cognitive impairment (MCI) grouped based on amyloid-β (Aβ) PET imaging into HCS−, HCS+ and MCI+. The proportion of individuals who were hetero- or homozygous for the *APOE* ε4 allele was higher in Aβ-positive groups than in Aβ-negative HCS, with one case of homozygous *APOE* ε4 genotype in HCS+. Normally distributed variables are summarized as mean with standard deviation (SD). Non-normally distributed variables are summarized as median with interquartile range (IQR). Group differences were calculated using parametric one-way ANOVA with Bonferroni's multiple comparison correction (for parameters 'Age', 'Years of education' and 'MMSE') or non-parametric Kruskal–Wallis test with false discovery rate (FDR) method of Benjamini and Hochberg (for parameters 'FMM Centiloid' and plasma biomarkers). The *P*-values for categorical variables such as 'Sex', '*APOE* ε4 carriers' and '*APOE* ε2 carriers' were calculated using Fisher's exact test. FMM = ^{18}F-flutemetamol; MMSE = Mini-Mental State Examination; NfL = neurofilament light; p-tau = phosphorylated tau.

preclinical AD) (Fig. 2A and Table 1). Following up on our previous reports,[18] we investigated whether $CD8^+$ TEMRA/effector cells were also increased in the CSF of individuals with early, preclinical AD. After mass cytometry analysis of CSF cells and paired PBMC samples from the same subjects, we applied automated cell clustering using FlowSOM and identified canonical immune cell populations, such as B cells, $CD4^+$ and $CD8^+$ T cells, myeloid cells (including monocytes and dendritic cells), innate lymphocytes [including natural killer (NK) cells], and unconventional T cells (including double-negative and γδ T cells) (Supplementary Fig. 1A–C). $CD4^+$ and $CD8^+$ T-cell clusters in CSF mainly exhibited an immune profile of memory cells with substantially lower amounts of naïve cells, as expected for CSF-derived cells[38] (Fig. 2B and C and Supplementary Fig. 1B). In line with our previous findings, we found that the relative abundance of $CD8^+$ TEMRA cells in CSF and in paired blood-derived PBMCs was increased in HCS+ compared to HCS− (Fig. 2D and E).

Next, we analysed study population 2, consisting of 30 study participants, which included both cognitively healthy HCS and individuals with MCI. Here, based on Aβ PET imaging data, we selected subgroups that were clearly Aβ-negative and strongly Aβ-positive (HCS−, HCS+, MCI+) to study the effect of high Aβ biomarker levels on the immune profile using mass cytometry and scRNA-seq (Fig. 1). Altered AD biomarker levels, hippocampal atrophy data, and details on *APOE* ε4 and ε2 genotypes are summarized in Supplementary Fig. 2A–W and Table 2.

Using CyTOF immunophenotyping for blood-derived PBMCs, we identified major immune cell populations (Supplementary Fig. 3A) with comparable proportions across diagnostic groups (Supplementary Fig. 3B). We then increased the resolution and identified canonical immune cell populations (here defined as 'landmark nodes') including subsets of B cells, $CD4^+$ and $CD8^+$ T cells, myeloid cells, innate lymphocytes, and unconventional T cells (Fig. 2F and G). We compared the proportions of landmark nodes across the three diagnostic groups and observed for $CD57^{low}$ $CD8^+$ TEMRA/effector cells an increased relative abundance in MCI+ ($P = 0.0027$) compared to HCS− (Fig. 2H).

Generally, proportions of peripheral immune cell subsets could be biased by subclinical levels of viral infections. Moreover, particularly herpesvirus infections have been suggested to be associated with AD pathogenesis.[39,40] Therefore, study participants were tested for elevated serum immunoglobulin (IgG and IgM) titres against CMV, EBV, HSV 1 and 2, and VZV. As expected, the majority of individuals were tested positive for IgG antibodies against EBV and VZV, while 40% of study subjects tested positive for anti-CMV IgG (Supplementary Fig. 3C). However, no significant differences in antiviral IgG serum titres between diagnostic groups were observed (Supplementary Fig. 3D). We controlled for an influence of herpesvirus infections on the abundances of canonical immune cell populations by correlating serum *Herpesviridae* IgG titres with landmark node abundances. Most *Herpesviridae* IgG titres had no influence on landmark node abundances (Supplementary Fig. 3E). However, anti-CMV IgG titres appeared to have significant effects on a number of landmark nodes, such as $CD4^+$ and $CD8^+$ memory T cells as well as on unconventional $CD56^+$ T cells (Supplementary Fig. 3E).

As the proportions of peripheral $CD8^+$ TEMRA/effector cells were also affected by anti-CMV IgG titres, we tested for CMV IgG-adjusted residuals to exclude that the observed difference was due to CMV reactivation. We confirmed the increase of $CD8^+$ TEMRA/effector landmark node abundance in MCI+ ($P = 0.0021$) compared to HCS−, even when corrected for a potential influence of CMV infections

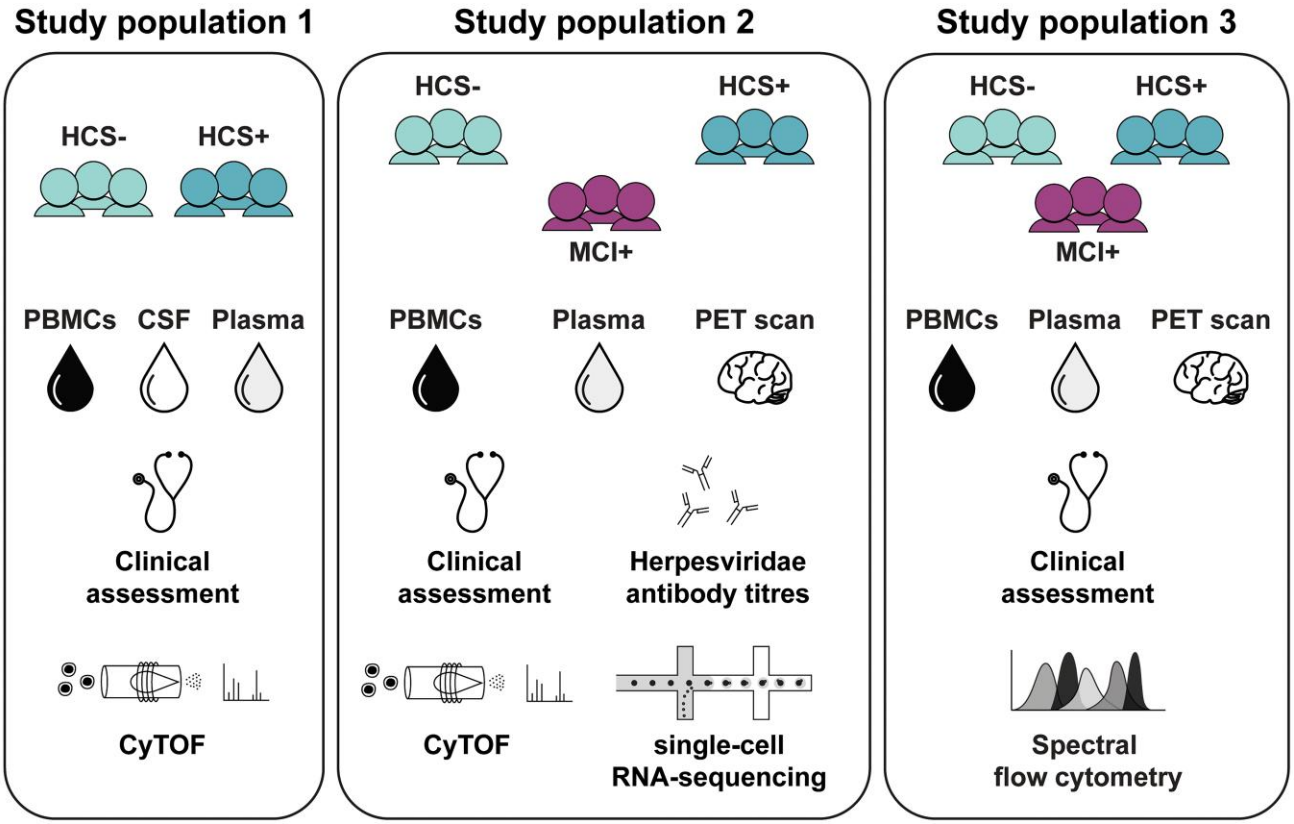

Figure 1 Study design for the analysis of T-cell reactivity in early Alzheimer's disease. In total, three study populations were analysed. Study participants were characterized using cognitive testing, amyloid-β (Aβ) PET imaging and fluid Alzheimer's disease (AD) biomarkers. Study population 1: Paired peripheral blood mononuclear cells (PBMCs) and CSF immune cells of AD biomarker-negative and -positive cognitively healthy subjects (HCS– and HCS+) were analysed via mass cytometry by time-of-flight (CyTOF). Study population 2: Individuals were divided into cerebral Aβ-negative and -positive cognitively healthy subjects (HCS– and HCS+), and Aβ-positive mild cognitive impairment (MCI+) subjects. PBMCs were analysed via CyTOF and single-cell RNA sequencing. Serum was used for quantification of anti-*Herpesviridae* antibody titres. Study population 3: Study participants were divided into HCS–, HCS+ and MCI+ groups. Functional analysis of T-cell secretome and epitope specificity was performed via spectral flow cytometry.

on $CD8^+$ TEMRA/effector cell abundances (Fig. 2I). Interestingly, in this study population, the comparison between HCS+ and HCS– did not reach statistical significance ($P = 0.1275$), in contrast to previous findings in other populations (Fig. 2D and E[18]). Frequencies of other T-cell subpopulations, including $CD4^+$ central memory (CM), $CD4^+$ effector memory (EM), regulatory T cells (Tregs) and unconventional T-cell subsets, were unchanged across the diagnostic groups after applying the adjustment for anti-CMV IgG titres (Supplementary Fig. 3F–J).

To associate $CD8^+$ TEMRA/effector immunophenotype with tau pathology, HCS and MCI subjects were subdivided in an alternative grouping according to the median of p-tau217 plasma levels (2.46 pg/ml) in study population 2 instead of using Aβ PET data. For readability, we refer to subjects above the median level as 'p-tau217+', emphasizing that this is not a clinical cut-off for tau biomarkers. $CD8^+$ TEMRA/effector cell abundance was increased in MCI p-tau217+ compared to HCS p-tau217–, which was also confirmed after adjustment for CMV IgG titres (Supplementary Fig. 3K and L).

Multiple linear regression analysis showed that the effects of age on $CD4^+$ and $CD8^+$ T-cell landmark node abundances were minor, with estimates close to 0 (Supplementary Fig. 3M). In addition, only the proportions of B and NK cell landmark nodes were affected by sex (Supplementary Fig. 3M).

Collectively, our data suggest an expansion of $CD8^+$ TEMRA/effector cells in peripheral blood and CSF of subjects in early AD stages, independent of latent *Herpesviridae* infections. Notably, these immune changes are already evident at the preclinical asymptomatic AD stage (HCS+).

Single-cell transcriptomics indicate less immunosuppression in early AD

We performed scRNA-seq for the same set of 30 PBMC samples from study population 2 to delineate the function of T lymphocytes in early AD at the transcriptional level. Overall, the scRNA-seq data analysis revealed comparable PBMC populations as in the previous mass cytometry data, including B cells, $CD4^+$ and $CD8^+$ T cells, innate lymphocytes, and myeloid cells (Fig. 3A and B). We did not find significant differences in relative abundances of main PBMC subsets (Supplementary Fig. 4A). Consistent with CyTOF-based surface characterization (Fig. 2F and G), we found $CD4^+$ naïve, memory, TEMRA/effector and Tregs within the $CD4^+$ T-cell compartment (Fig. 3C and D). Interestingly, while the relative abundance of $CD4^+$ Tregs was unchanged across diagnostic groups (Fig. 3E and Supplementary Fig. 3H), gene set enrichment analysis (GSEA) on this subset revealed significantly decreased enrichment scores for pro-inflammatory (TNF and IL-6 signalling), immunosuppression-related (TGFβ signalling) and Treg maturation-related (IL-2 and STAT5 signalling) gene modules, and in parallel increased scores for anergy-related gene modules in HCS+ compared to HCS– (Fig. 3F and Supplementary Table 1).

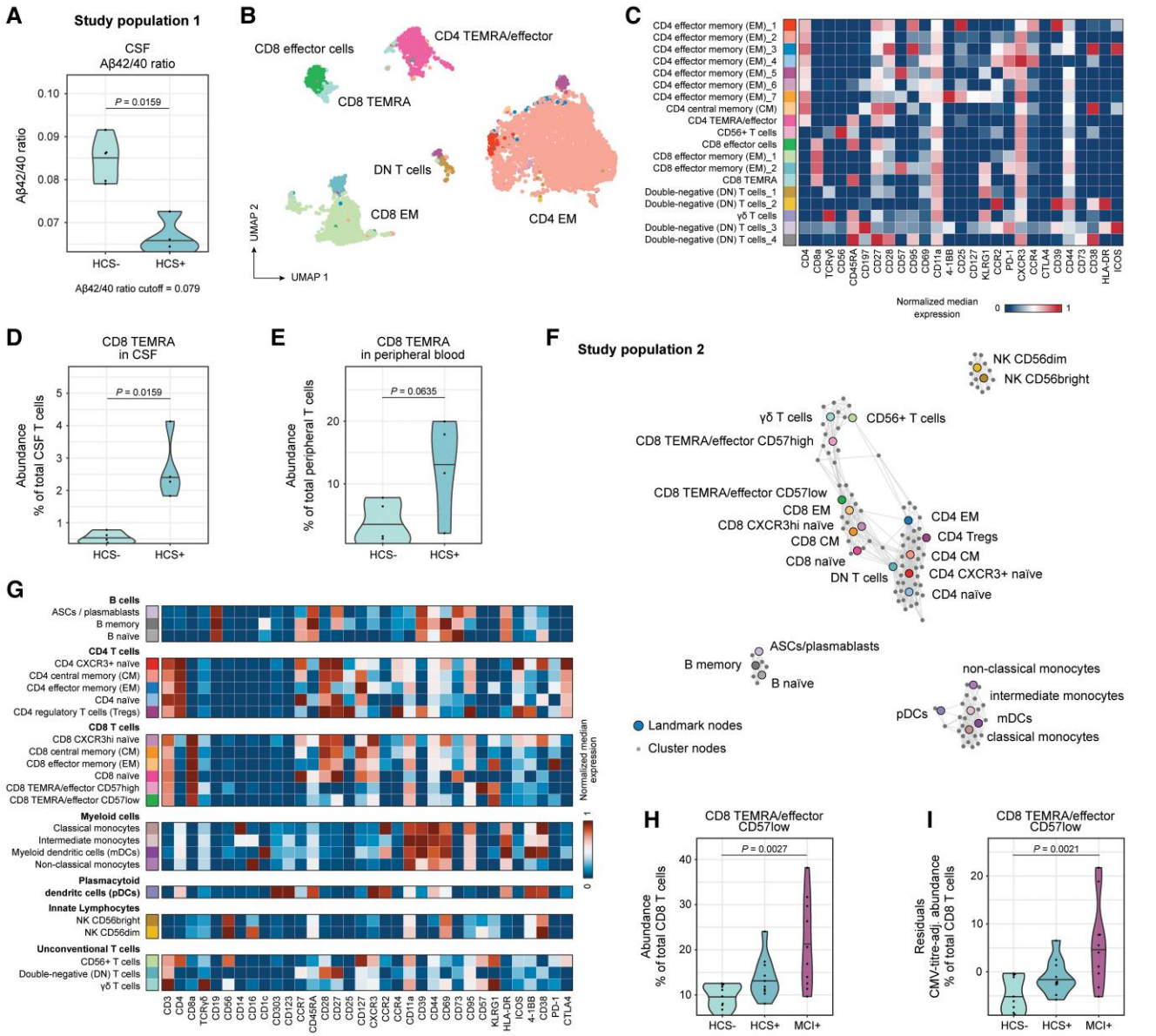

Figure 2 Increased abundance of CD8⁺ TEMRA cells in CSF and blood of amyloid-β-positive individuals. (**A**) Study population 1: Violin plot depicting CSF amyloid-β $(Aβ)_{42/40}$ ratio in cognitively healthy subjects (HCS). Subjects were categorized as biomarker-positive if $Aβ_{42/40}$ ratio in CSF was below threshold value (HCS+, cut-off = 0.079). (**B**) Uniform manifold approximation and projection (UMAP) coloured by CSF T-cell subsets obtained with FlowSOM clustering for all non-naïve CD3⁺ cells in the CSF. (**C**) Corresponding heat map depicting median scaled marker expression within CSF T-cell subsets. (**D**) Violin plot showing relative abundance of CD8⁺ TEMRA cells among total CSF T cells. (**E**) Violin plot showing relative abundance of CD8⁺ TEMRA cells among total peripheral T cells. (**F**) Study population 2: Scaffold map of total CD45⁺ cells analysed via mass cytometry by time-of-flight (CyTOF). Each node represents a cell cluster, including landmark nodes (manually annotated and merged FlowSOM clusters, shown in colours) and cluster nodes (unsupervised FlowSOM clusters, in grey). (**G**) Corresponding heat map depicting median scaled marker expression within each landmark node. (**H**) Violin plot showing relative landmark node abundance for the CD8⁺ TEMRA/effector CD57low node among total CD8⁺ T cells. (**I**) Violin plot showing anti-CMV (Cytomegalovirus) IgG-adjusted landmark node abundance for the CD8⁺ TEMRA/effector CD57low node among total CD8⁺ T cells. Statistical significance was calculated using non-parametric unpaired Wilcoxon rank-sum test (**A**, **D** and **E**), or non-parametric Kruskal–Wallis test with false discovery rate (FDR) method of Benjamini and Hochberg (**H** and **I**). Selected *P*-values ≤ 0.1 (FDR 10%) are displayed. DN = double negative; EM = effector memory cell; HCS− = Aβ-negative healthy control subjects; MCI+ = Aβ-positive mild cognitive impairment; mDC = myeloid dendritic cell; NK = natural killer cell; pDC = plasmacytoid dendritic cell; TEMRA = T effector memory cells re-expressing CD45RA.

Conversely, MCI+ displayed an increased enrichment score for pro-inflammatory (IL-6 signalling) and a decreased enrichment score for the immunosuppression-related gene module (TGFβ signalling) compared to HCS− (Fig. 3F). In the CD8⁺ T cell compartment, we identified CD8⁺ activated naïve, naïve, memory and TEMRA/effector cells (Fig. 3G and H). Single-cell transcriptomics also confirmed the increase of the CD57low CD8⁺ TEMRA/effector cell cluster in MCI+ compared to HCS− (Fig. 3I). For this cluster, GSEA showed significantly decreased scores for pro-inflammatory gene modules (inflammatory response, TNF and IL-6 signalling) in CD57low CD8⁺ TEMRA/effector cells of HCS+ compared to HCS−. In contrast, we observed increased enrichment scores of pro-inflammatory gene modules and simultaneously decreased cytotoxicity-related gene modules in MCI+ compared to HCS−

(Fig. 3J and Supplementary Table 1). As for the mass cytometry data, age and sex differences had only minor influences on landmark cluster abundances, with estimates close to 0 in a multiple linear regression analysis (Supplementary Fig. 4B).

Taken together, the single-cell transcriptional profiling of $CD4^+$ and $CD8^+$ T-cell populations in the blood of subjects with early AD indicates a possible impairment of $CD4^+$ Treg function and peripheral tolerance in the preclinical AD stage (HCS+). Potentially, this could provide the basis for developing adaptive immune responses against auto-antigens, such as Aβ-based aggregates in preclinical AD. On the other hand, in MCI+, a less immunosuppressive Treg and a more pro-inflammatory $CD8^+$ TEMRA/effector transcriptomic signature appear to accompany neurodegeneration, as indicated by elevated plasma NfL levels (Supplementary Fig. 2F and G), reduced hippocampal volumes (Supplementary Fig. 2J–M), and the onset of cognitive decline.

Altered T-cell reactivity against linear amyloid-β peptide in early AD stages

To investigate the functional component of T cells in the early AD continuum, we analysed the T-cell secretome and reactivity against AD pathology-related antigen pools. For this, we used PBMCs from study population 3, consisting of 44 study participants, which includes HCS and MCI subjects grouped based on Aβ PET imaging into cerebral Aβ-negative and Aβ-positive subjects (Table 3). An overview of altered AD biomarker levels and *APOE* ε4 and ε2 genotype information is provided in Supplementary Fig. 5A–S and Table 3.

We first measured the production of cytokines and cytolytic molecules per single cell for *ex vivo* reactivated T cells via spectral flow cytometry (Fig. 4A). We identified $CD4^+$ and $CD8^+$ T-cell subsets via automated FlowSOM clustering (Fig. 4B and C). Within these subsets, we used activation markers, cytokines and cytolytic molecules to obtain clusters with specific patterns of activation state and secretome. For $CD4^+$ EM T cells, we identified seven functional clusters (Fig. 4D). A pro-inflammatory $CD4^+$ EM T-cell cluster containing high levels of Interferon-gamma (IFN-γ) ($CD4^+$ EM Cluster 1) was decreased in HCS+ and MCI+ groups compared to HCS− (Fig. 4E). In contrast, $CD4^+$ EM Clusters 3, 4 and 5 showed an activation pattern with increased expression of immune homeostasis-related Fas-receptor (CD95) and with higher expression of the immune checkpoint 'programmed cell death receptor 1′ (PD-1) ($CD4^+$ EM Cluster 3) or production of type 2 T helper (T_H2) cell-related cytokines such as IL-4 and IL-13 ($CD4^+$ EM Clusters 4 and 5). The frequency of these clusters was increased in HCS+ subjects compared to HCS− and MCI+ (Fig. 4F–H). For $CD4^+$ CM T cells, we identified eight functional clusters, of which $CD4^+$ CM Cluster 6 displayed a pro-inflammatory immune signature with high levels of IFN-γ and decreased frequency in HCS+ compared to HCS− (Fig. 4I and J). For $CD8^+$ TEMRA/effector cells, we identified eight functional clusters (Supplementary Fig. 6A). Of these, $CD8^+$ TEMRA/effector Cluster 8 showed a $CD95^+$ activation pattern with high expression of inhibitory immune checkpoint marker CTLA-4, as well as anti-inflammatory cytokines IL-4, IL-10 and IL-13. This cluster was reduced in MCI+ compared to HCS− and HCS+ (Supplementary Fig. 6B).

For investigating the antigen specificity of T cells, we employed an *in vitro* antigen presentation assay in which we pulsed PBMCs with peptide pools of AD pathology-related putative antigens or positive control antigens derived from influenza, CMV and EBV viruses (Fig. 5A). As readout, we measured the surface expression of T-cell markers for antigen-specific activation via spectral flow cytometry (Fig. 5A). Peptide pools of putative antigen candidates were designed using different approaches including limited proteolysis (LiP) and *in silico* predictions. A previously described source of AD-related peptide antigens is the $Aβ_{1-42}$ peptide,[21] the major component of Aβ fibrils and Aβ plaques. To uncover regions of Aβ fibrils that are more prone to structure-dependent digestion and potential presentation to T cells by antigen-presenting cells (APCs), we performed LiP for Aβ fibrils. We produced Aβ fibrils and partially digested them *in vitro* using Proteinase K, a broad-specificity protease that cleaves proteins in a structure-dependent manner[41] (Supplementary Fig. 6C and D). With this approach, we found that the N-terminus of $Aβ_{1-42}$ peptide had a higher density of half-tryptic sites, indicating increased structure-dependent digestion while being located within the Aβ fibril (Supplementary Fig. 6E). Conversely, the mid-sequence and C-terminus were structurally less accessible for Proteinase K and more hidden within the Aβ fibril. Due to the different accessibility of $Aβ_{1-42}$ peptide regions within the fibril, we included peptide pools deriving from the linear $Aβ_{1-42}$ divided into N-terminal, mid-sequence and C-terminal pools (Supplementary Table 2). In addition, we included a peptide pool deriving from full-length 2N4R tau and axonal 0N4R tau variant representing both AD- and neurodegeneration-related antigens.[42] For the tau pool, we selected linear peptides showing higher predicted affinity towards HLA molecules using the NetMHCIIpan database[43,44] (Supplementary Fig. 6F). Moreover, tau-derived autoantigens have already been described in the general population, therefore we also tested tau peptides, which have previously been shown to have the highest percentage of total T-cell responses[45] (Supplementary Table 3). All selected peptides were 15-mers, which are preferentially presented by HLA class II to $CD4^+$ T cells.

We tested our antigen candidates with a subset of study population 3 that contained cerebral Aβ-negative and -positive HCS and MCI subjects (Supplementary Fig. 7A). First, we compared positive control antigens with unpulsed conditions and selected optimal co-stimulatory readout parameters for $CD4^+$ EM (OX40) and CM (4-1BB, CD25hi and OX40) T cells (Fig. 5B and C and Supplementary Fig. 7B–D). Compared to the unpulsed condition, we identified autoreactive $CD4^+$ EM and CM T cells responsive to Aβ mid-sequence and C-terminus, but not to N-terminal Aβ or tau pools. This reactivity was most pronounced in HCS+ and, to a lesser extent, in HCS− subjects (Fig. 5B and C and Supplementary Fig. 7C). These results stood in contrast to the LiP findings, which indicated that the Aβ N-terminus is most accessible for antigen processing and presentation, suggesting the involvement of immune tolerance towards the Aβ N-terminus. In addition, $CD4^+$ EM and CM T cells from MCI+ subjects generally exhibited decreased reactivity to all peptide pools tested within the same reaction time and under the same conditions as cells from HCS individuals, displaying only weak reactivity against Aβ mid-sequence peptide pool (Fig. 5B and C and Supplementary Fig. 7C). Focusing solely on MCI-derived cells across different stimulations reinforced this notion of diminished antigen reactivity in MCI+, extending even to positive control antigens (Supplementary Fig. 7E–H).

In summary, we report that compared to MCI, the preclinical AD stage (HCS+) is characterized by T cells with a less pro-inflammatory but more T_H2 response-related immune profile. Moreover, $CD4^+$ memory T cells showed an intact antigen-specific response to Aβ-derived linear peptide epitopes in cognitively healthy subjects, but less so in Aβ-positive MCI subjects. Specifically, this immune response is directed against the mid-sequence and C-terminal fragments of the Aβ peptide. This

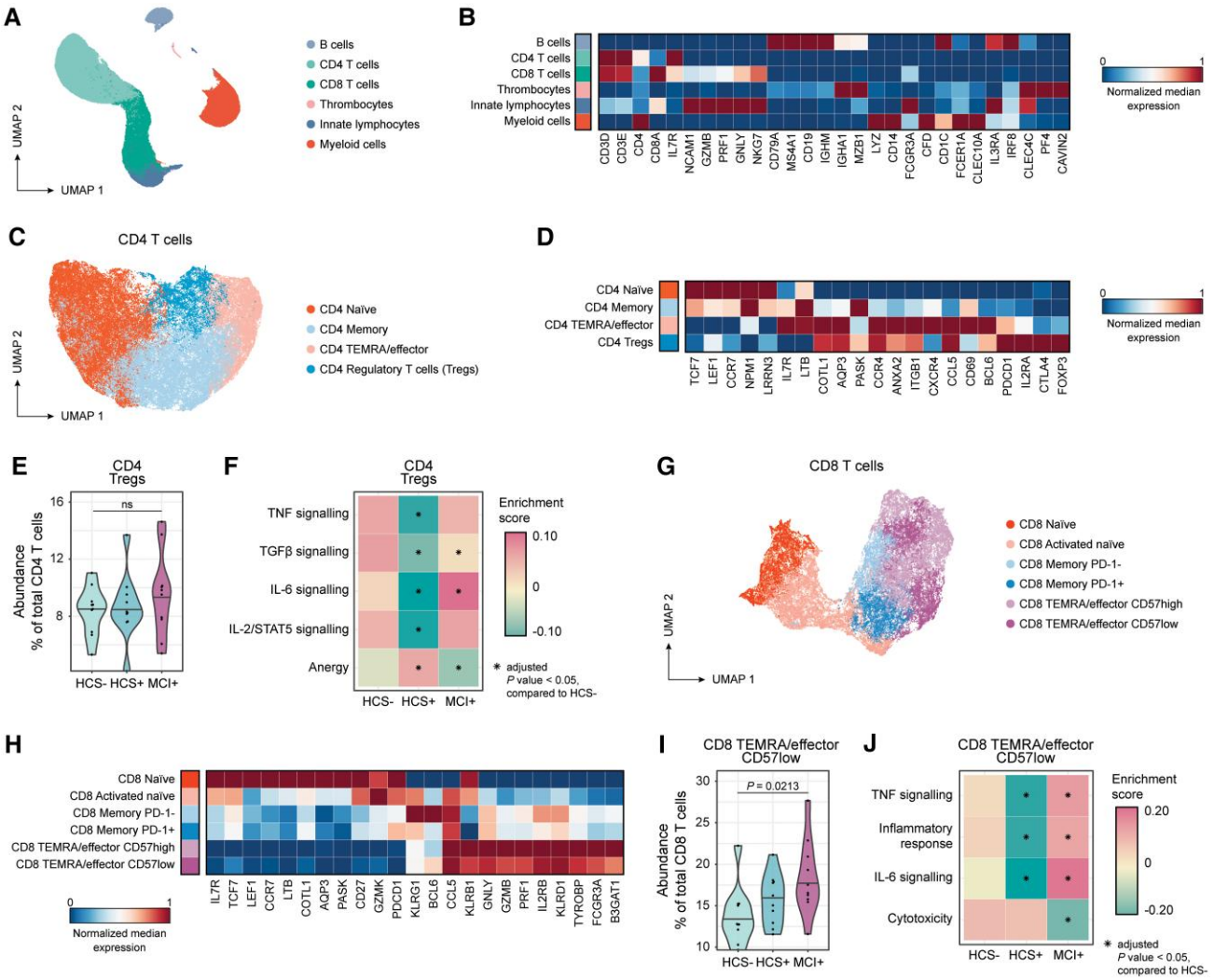

Figure 3 Single-cell RNA sequencing analysis reveals downregulated CD4⁺ Treg gene signatures in preclinical Alzheimer's disease. (**A**) Uniform manifold approximation and projection (UMAP) of total peripheral blood mononuclear cells (PBMCs) in single-cell RNA sequencing (scRNA-seq) data, coloured by cluster assignment according to unsupervised graph-based clustering with Louvain algorithm. (**B**) Heat map depicting scaled gene expression within each PBMC cluster. (**C**) UMAP of CD4⁺ T-cell sub-clusters in scRNA-seq data coloured by cluster assignment according to unsupervised graph-based clustering with Louvain algorithm. (**D**) Heat map depicting scaled gene expression within each CD4⁺ T-cell subcluster. (**E**) Violin plot showing relative abundance of CD4⁺ regulatory T cells (Tregs) among total CD4⁺ T cells. (**F**) Heat map depicting enrichment scores for CD4⁺ Tregs in the three diagnostic groups for selected gene sets. (**G**) UMAP of CD8⁺ T-cell sub-clusters coloured by cluster assignment according to unsupervised graph-based clustering with Louvain algorithm. (**H**) Heat map depicting scaled gene expression within each CD8⁺ T-cell subcluster. (**I**) Violin plots showing relative abundance of CD8⁺ TEMRA/effector CD57low cluster among total CD8⁺ T cells. (**J**) Heat map depicting enrichment scores for the CD8⁺ TEMRA/effector CD57low cell cluster in the three diagnostic groups for selected gene sets. For relative abundance, statistical significance was calculated using non-parametric Kruskal–Wallis test with false discovery rate (FDR) method of Benjamini and Hochberg. Selected *P*-values ≤ 0.1 (FDR 10%) are displayed. HCS+/− = Aβ-positive/negative healthy control subjects; MCI+ = Aβ-positive mild cognitive impairment; TEMRA = T effector memory cells re-expressing CD45RA.

combined immunological framework could theoretically favour a protective adaptive immune response against pathological compounds in preclinical AD.

Discussion

This study provides an in-depth analysis of the adaptive immune system in early AD by using state-of-the-art single-cell techniques, such as multidimensional mass cytometry combined with gene expression analysis via scRNA-seq, as well as single-cell secretome analysis and antigen presentation assays. Moreover, the study populations from the early AD continuum used here are characterized in terms of neuropsychological assessment, cerebral Aβ status, blood-based AD biomarkers, and anti-viral antibody titres.

With this work, we show that peripheral and cerebral adaptive immune cell changes are functionally distinct in individuals in the early stages of AD. These early stages include preclinical AD (Aβ-positive and cognitively healthy) and Aβ-positive MCI. For the CD8⁺ subtype of T cells, we found substantially increased frequencies of TEMRA/effector cells in the blood of MCI cases and even in the CSF of preclinical AD cases, but their target antigens still remain elusive. Moreover, these cells proved to have a less pro-inflammatory transcriptomic signature in preclinical AD, a

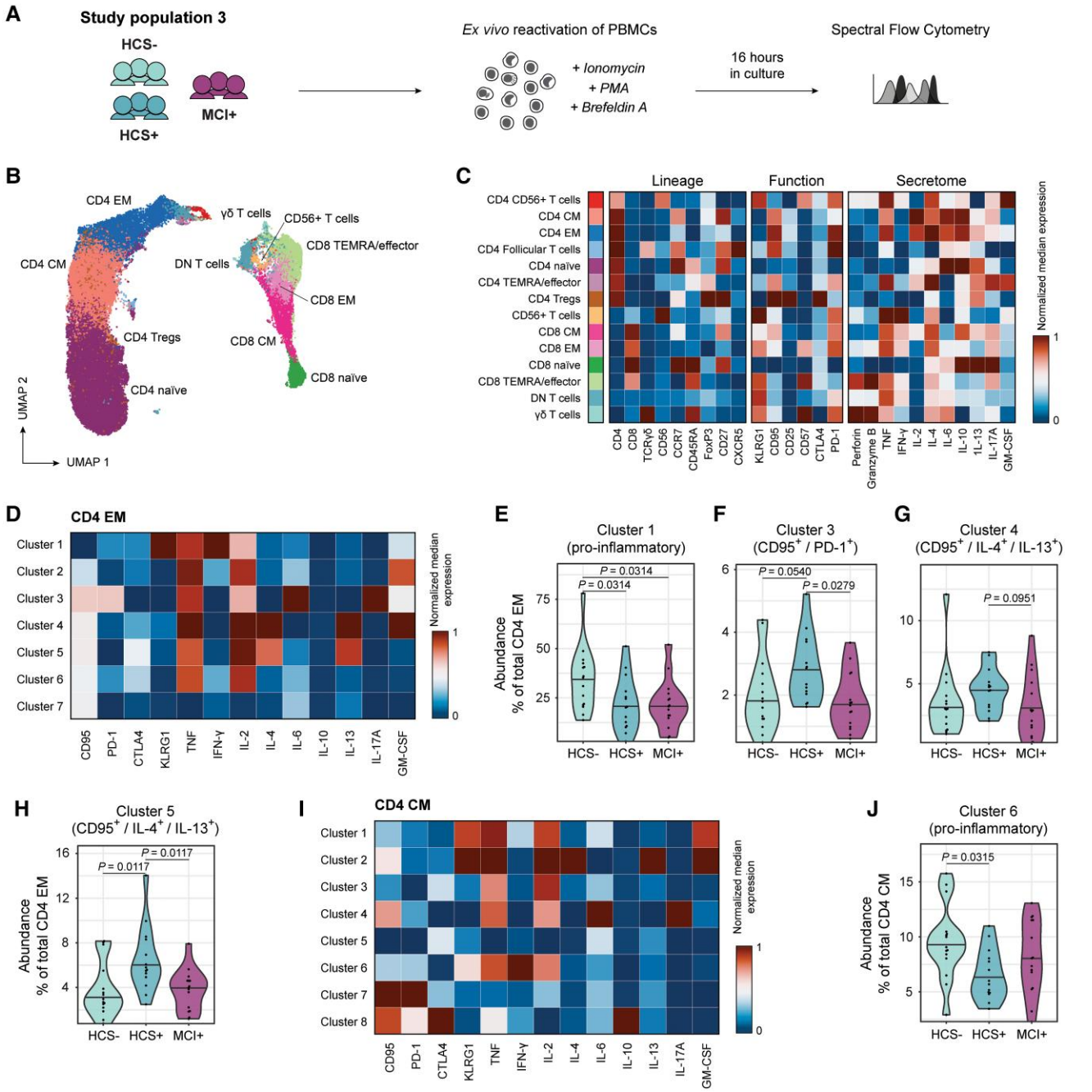

Figure 4 Secretome analysis reveals type 2 T helper-related and anti-inflammatory T-cell profiles in preclinical Alzheimer's disease. (**A**) Study population 3: Peripheral blood mononuclear cells (PBMCs) were reactivated *ex vivo*, T-cell secretome was analysed via spectral flow cytometry. (**B**) Uniform manifold approximation and projection (UMAP) of total T cells coloured by cluster assignment based on unsupervised FlowSOM clustering. (**C**) Corresponding heat map depicting scaled median expression within each T-cell cluster. (**D**) Heat map depicting scaled median expression for activation markers and cytokines to identify seven functional clusters of CD4$^+$ effector memory (EM) cells (using automated FlowSOM clustering). (**E–H**) Violin plots showing relative abundance of Cluster 1 (**E**), Cluster 3 (**F**), Cluster 4 (**G**) and Cluster 5 (**H**) among total CD4$^+$ EM cells. (**I**) Heat map depicting scaled median expression for activation markers and cytokines to identify eight functional clusters of CD4$^+$ central memory (CM) cells (using automated FlowSOM clustering). (**J**) Violin plot showing relative abundance of Cluster 6 among total CD4$^+$ CM cells. Statistical significance was calculated using non-parametric Kruskal–Wallis test with false discovery rate (FDR) method of Benjamini and Hochberg. Selected *P*-values ≤ 0.1 (FDR 10%) are displayed. DN = double negative; HCS+/– = Aβ-positive/negative healthy control subjects; MCI+ = Aβ-positive mild cognitive impairment; TEMRA = T effector memory cells re-expressing CD45RA.

pattern that appeared to reverse in individuals at a more advanced disease stage, i.e. Aβ-positive MCI. A different picture emerged for the CD4$^+$ T helper and Treg subtype. Here, we observed a less immunosuppressive gene profile for Tregs in preclinical AD and MCI, leaving still the possibility of successfully mounting beneficial adaptive immune responses in preclinical AD. And indeed, functional analyses show that CD4$^+$ memory T cells from preclinical AD subjects display a more T_H2-like phenotype, secrete B cell-stimulating cytokines, such as IL-4, and react against Aβ-derived antigens *in vitro*. In particular, our study demonstrates the presence

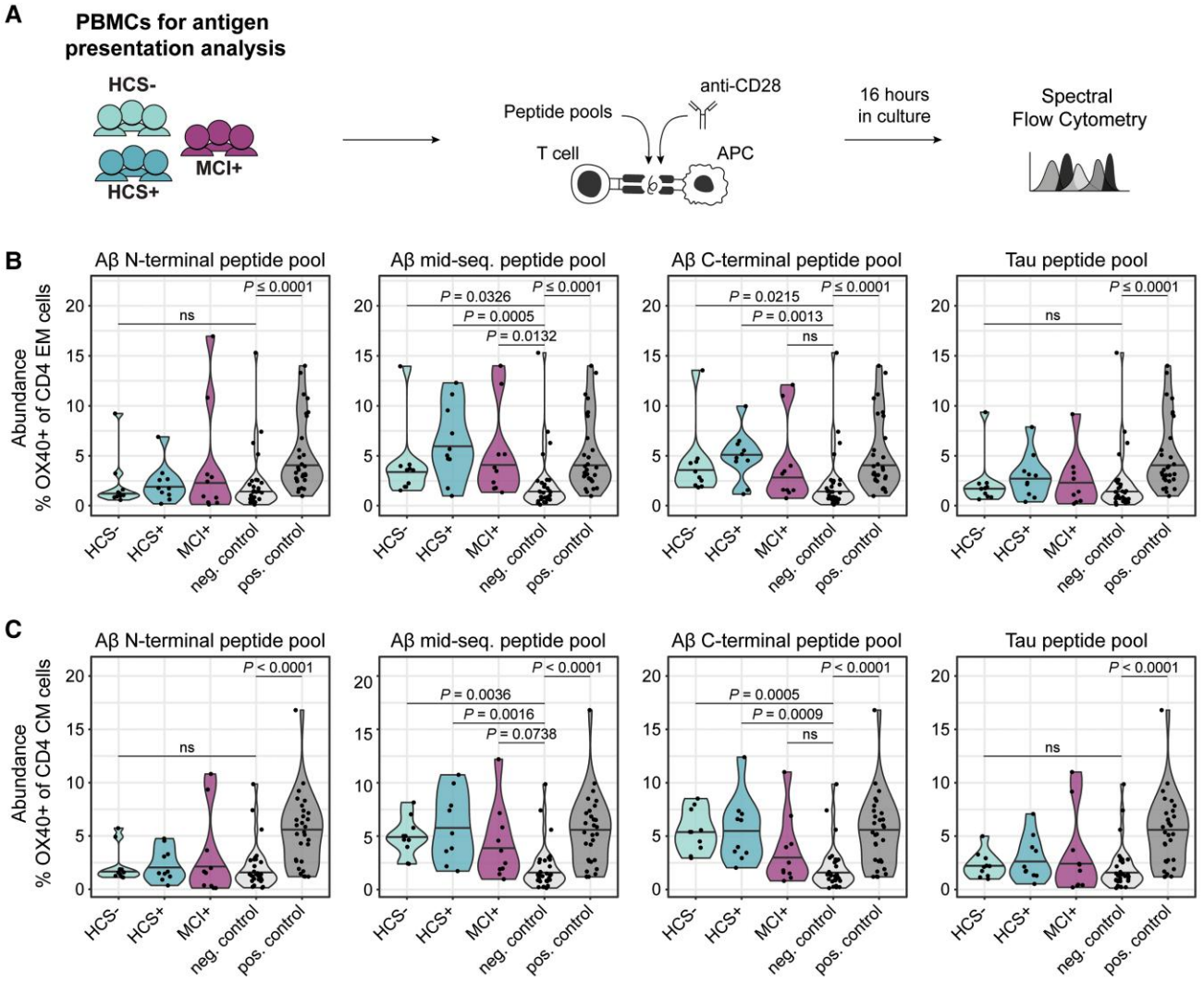

Figure 5 Altered T-cell reactivity towards Alzheimer's disease (AD)-related peptide epitopes in early AD stages. (**A**) Peripheral blood mononuclear cells (PBMCs) from a subset of 30 subjects from study population 3 were pulsed for 16 h with anti-CD28 agonistic antibody and AD-related peptide pools. Expression of antigen-specific T-cell markers were measured via spectral flow cytometry. (**B** and **C**) Violin plots depicting the relative abundance of $OX40^+$ cells among total $CD4^+$ effector memory (EM) (**B**), and total $CD4^+$ central memory (CM) (**C**) T cells, comparing diagnostic groups after pulsing with AD-related peptide pools. Positive and negative control data were pooled from all study groups. The *P*-values indicate statistical significance by comparison with unpulsed negative control. Statistical significance was calculated using non-parametric Kruskal–Wallis test with false discovery rate (FDR) method of Benjamini and Hochberg. Selected *P*-values ≤ 0.1 (FDR 10%) are displayed. Aβ = amyloid-β; APC = antigen-presenting cell; HCS+/– = Aβ-positive/negative healthy control subjects; MCI+ = Aβ-positive mild cognitive impairment.

of autoreactive $CD4^+$ memory T cells preferentially targeting mid-sequence and C-terminus regions of the $A\beta_{1\text{-}42}$ peptide. However, the more advanced MCI disease stage appeared to be characterized by less immunoreactivity, as any antigen-specific immune response previously seen in the cognitively healthy stage was no longer evident. Importantly, we show that our immunophenotyping results are independent of latent background infections with widespread *Herpes viridae*.

In line with our previous studies,[18] we observed an increased abundance of $CD8^+$ TEMRA/effector cells in peripheral blood and CSF of individuals in the early AD continuum. Similar results have previously been reported for CSF-derived cells from patients with MCI and AD.[14] As for other neurodegenerative diseases, increased numbers and clonal expansion of $CD8^+$ TEMRA cells have also been observed in amyotrophic lateral sclerosis type 4 (ALS4) patients, suggesting their general involvement in neurodegeneration.[46] In our study, the increased expression of pro-inflammatory gene modules in $CD8^+$ TEMRA/effector cells of MCI subjects in combination with less immunosuppressive Treg function might indicate a contribution of $CD8^+$ TEMRA/effector cells to the general hyper-inflammatory environment observed in MCI and AD. Indeed, a study using *in vitro* 3D modelling of the human brain showed increased infiltration of $CD8^+$ T cells into AD brain cultures accompanied by exacerbated neuroinflammation and neurodegeneration.[47] Compared to Aβ pathology, accumulation of neurofibrillary tangles made of hyperphosphorylated tau is more associated with neurodegeneration and cognitive decline.[48] In line with this, in a previous study we also found increased numbers of $CD8^+$ TEMRA/effector cells in individuals with high plasma levels of p-tau181.[18] This finding was replicated in the present study in MCI subjects with elevated plasma levels of p-tau217, an AD biomarker that correlates more strongly with brain Aβ and paired helical filament tau (PHFtau) tangles than p-tau181.[49] Moreover, recent studies suggest the involvement of $CD8^+$ T cells in tau pathology,

potentially driving neurodegeneration in response to tau-derived antigens.[50,51] To better associate CD8$^+$ TEMRA/effector immunophenotyping data with tau pathology, future studies and follow-up assessments will have to include more specific biomarkers tracking tau aggregation, such as tau PET or fluid biomarker candidates, such as MTBR-tau243.[52] In future studies, we will design peptide pools deriving from the major components of AD pathology, Aβ and tau, and other sources that are preferentially presented to CD8$^+$ T cells. To date, we have not found specific responses of CD8$^+$ TEMRA/effector cells against AD-related (auto)antigens, but antigen presentation setups optimized for CD8$^+$ T cells will address this matter. Importantly, one might have to also consider other CD8$^+$ T-cell subtypes that might be involved in AD pathology, e.g. potentially beneficial, suppressive CD8$^+$ PD-1$^+$ T cells that might help shut down hyper-inflammatory microglia.[53] In most cases, cytotoxic CD8$^+$ T cells are known to react against cytoplasm-derived antigens such as viral or tumour antigens. CD8$^+$ T cells reacting against viral epitopes have been detected in ALS, Parkinson's disease (PD) and AD patients.[14,46,54] Virus infections could trigger the activation of cross-reactive T cells via molecular mimicry and antigen-independent bystander activation,[55] and indeed the existence of cross-reactive T cells has been suggested in multiple sclerosis and narcolepsy.[56-58]

For CD4$^+$ T cells, we observed an intact reactivity to Aβ-derived epitopes in the mid-sequence and C-terminus of A$\beta_{1\text{-}42}$ peptide in cognitively healthy individuals with and without cerebral Aβ burden. This was evidenced by the increased frequency of CD4$^+$ memory T cells expressing antigen-specific co-stimulatory immune checkpoints OX40 and 4-1BB, both members of the tumour necrosis factor receptor superfamily. Conversely, we observed no reactivity towards Aβ N-terminus peptide pool. Previous studies reported increased T-cell reactivity against Aβ-derived antigens in AD patients and age-matched cognitively healthy subjects.[20,21] However, these studies did not perform a detailed AD biomarker analysis, namely Aβ PET scan and AD blood-based biomarkers. The lack of reactivity towards N-terminal fragments of Aβ suggests that autoreactive T cells against the Aβ N-terminus might be subjected to peripheral tolerance. Originally, upon cleavage of transmembrane self-protein APP by α- and γ-secretase in the non-amyloidogenic pathway, Aβ N-terminus is released within the sAPPα fragment and Aβ mid-sequence/C-terminus is part of the p3 peptide, making both available for processing and antigen-presentation by APCs, and ultimately for induction of peripheral immune tolerance.[59] In contrast, A$\beta_{1\text{-}42}$ peptide is a product of the amyloidogenic pathway, and during oligomerization and fibril formation, the C-terminus is located within the internal and hidden part of the Aβ fibril, and thus less accessible for structure-dependent digestion by APCs.[60-62] This could result in autoreactive T cells specific for the C-terminus of A$\beta_{1\text{-}42}$ that escape tolerance during AD pathology. As the N-terminal segment is located on the external and more accessible part of the Aβ fibril, it is prone to structure-based digestion,[60] as shown by the LiP results. Hence, epitopes residing in the N-terminal segment might be preferentially presented by APCs and continue to induce strong peripheral tolerance, which might prevent a successful T-cell response against N-terminal A$\beta_{1\text{-}42}$.

The topic of immune tolerance in AD has been the subject of controversial debates. On the one hand, there are voices calling for therapeutic approaches that can limit immunosuppression and thus enable the adaptive immune system to act more effectively against pathological features of AD. Breaking immune tolerance using approaches such as immune checkpoint blockade of PD-1 or PD-1 ligand (PD-L1) in β-amyloidosis and tauopathy mouse models was shown to cause a systemic immune response, recruiting monocyte-derived macrophages to the brain, and resulting in reduced AD-associated pathology.[63,64] Interestingly, blockade of the immune checkpoint in these experiments resulted not only in mobilization of monocytes to the brain but also in additional recruitment of CD4$^+$ Tregs,[50,65] suggesting that targeting PD-1 also alleviates the suppression of Tregs. On the other hand, enhancing local CD4$^+$ Treg populations, particularly in the meninges, may help restrict effector cell infiltration into the brain and, in turn, mitigate neuroinflammation.[66] It has been postulated that in common autoimmune diseases, but also in AD, it may be necessary to enhance Treg expansion and immunomodulatory function, e.g. by *ex vivo* expansion or *in vivo* treatment with IL-2.[67-70] Ultimately, both approaches appear to result in increased immunomodulatory potential of Tregs, which would be optimal for containing hyperinflammation and potentially harmful CD8$^+$ T-cell responses in later AD stages, but they do not solve the problem of apparently suppressed beneficial T-cell responses in preclinical AD. The duality of these T-cell responses may help explain why certain immunosuppressive strategies in AD (e.g. broad steroid medication, such as prednisone) have yielded disappointing results,[71] as they may inadvertently inhibit both harmful and protective immune pathways.

CD4$^+$ memory T cells displayed increased reactivity to AD-related antigens, particularly in cognitively healthy subjects, while MCI subjects showed a general decrease in T-cell immunoreactivity. In line with these results, studies using mouse models of β-amyloidosis showed that infiltrating T cells in brains with advanced Aβ pathology produced less pro-inflammatory cytokines.[72,73] Indeed, we observed lower frequencies of T helper cell subsets producing IL-4 and IL-13 in Aβ-positive MCI, which could result in less stimulation of antibody-producing B cells[74-76] and therefore less immunoglobulins potentially opsonizing Aβ plaques for clearance. Considering that Aβ accumulation in the brain begins decades before the onset of AD-related symptoms,[2,77] T-cell hypo-responsiveness in Aβ-positive MCI might also be caused by exhaustion due to chronic antigen exposure. We reported previously that antigen presentation by myeloid-derived phagocytes is impaired under Aβ stress *in vitro* and *ex vivo* in brain-derived APCs from β-amyloidosis mouse models.[73] Impaired myeloid-derived phagocyte function and Aβ clearance might be among the causes for dysfunctional antigen presentation and subsequent reduced T-cell activation observed in AD patients and β-amyloidosis mouse models.[72,73,78]

In light of generally increased numbers and the more pro-inflammatory gene expression profile of CD8$^+$ TEMRA/effector cells in Aβ-positive MCI, this may be further evidence that CD8$^+$ T cells are involved in AD pathology or neurodegeneration, possibly through their contribution to neuroinflammation. Interestingly, this CD8$^+$ T-cell gene expression profile aligns with recent findings on brain-resident CD8$^+$ memory T cells in a mouse model of β-amyloidosis, which exhibited transcriptomic features reminiscent of CD8$^+$ T cells in acute viral infection models, also without an accompanying upregulation of cytotoxic markers.[79] Without knowledge of the target antigen, it remains speculative whether their role is beneficial or harmful. Moreover, in the absence of specific antigenic stimulation, we have not yet fully captured the pro-inflammatory secretome in our functional assays. However, their pro-inflammatory nature at the transcriptomic level suggests that CD8$^+$ T cells, particularly TEMRA/effector cells, may further drive and exacerbate neuronal loss if responsive to antigens associated with AD pathology or neurodegenerative processes, and if they reach the CNS in their activated state.[47,50] Considering the fact that potential target antigens for these

$CD8^+$ T cells would first occur in the CNS, early changes in the $CD8^+$ T-cell compartment in the CSF could already arise in the preclinical stage of AD, as observed in this study. Nevertheless, the immune setup in preclinical AD still appears to be favourable for potentially beneficial $CD4^+$ T cells targeting Aβ, because peripheral immunosuppression is downregulated in general, and $CD4^+$ memory T cells show antigen-specific responses. This could, in theory, favour clearance of pathological Aβ aggregates via B cell stimulation. However, as $CD4^+$ T-cell specificity is aimed at parts of Aβ that are more hidden within the aggregated fibril structure, this response might miss its target. In fact, most Aβ-targeting antibodies, which have been tested to successfully elicit plaque clearance, bind epitopes within or near the N-terminus of the Aβ peptide.[80-82] In contrast, T-cell responses against the N-terminus of Aβ appear to be suppressed. Thus, there could be an epitope mismatch that complicates proper $CD4^+$ T-cell stimulation in preclinical AD. Future studies focusing on Tregs and peripheral tolerance in preclinical AD might provide further insight into this matter.

It is important to mention that our antigen candidate pools were not exhaustive, and in addition, the selection of peptide epitope candidates was quite stringent for long proteins, such as tau, selecting only peptides with high affinity for HLA molecules. Potential autoantigens, however, might have lower HLA affinity to escape immune tolerance mechanisms. Moreover, to date we have mainly considered linear peptide antigens without modifications. But especially tau, with its multitude of post-translational modifications, such as phosphorylations at multiple sites, might harbour more potential T-cell epitopes. Thus, our findings do not exclude the possibility of relevant tau-specific immune responses, but we did not observe such tau-specific responses in this study.

Conclusions

This research sheds light on the complex immunological changes in early AD stages, underscoring the importance of developing both tailored immunomodulatory therapies and reliable immune-related biomarkers for more nuanced intervention strategies. While it might be important in preclinical AD to support potentially beneficial $CD4^+$ T-cell immune responses, it may become necessary in later stages to block potentially harmful T-cell responses that otherwise aggravate neuroinflammation and neurodegeneration. To determine which immune responses are truly protective over time, it will be crucial to conduct long-term longitudinal studies.

Data availability

The datasets used and analysed during the current study are available from the corresponding author on reasonable request after evaluation by the authors and, if applicable, by the local ethics authority. The code generated during this study for data analysis is publicly available at Zenodo (CERN, European Organization for Nuclear Research) under https://doi.org/10.5281/zenodo.13270921.

Acknowledgements

We would like to thank all the volunteers who kindly participated in the studies. We thank all study physicians and neuropsychologists for their contribution to the assessments and conduct of the study. Samples from participants were collected at the Center for Prevention and Dementia Therapy (Institute for Regenerative Medicine, University of Zurich) by study nurses led by Esmeralda Gruber. We would like to thank the Cytometry Facility (University of Zurich) for technical assistance, and the Institute of Medical Virology (University of Zurich) for virus serology analysis. Special thanks go to Prof. Paola Picotti from the Institute of Molecular Systems Biology (ETH Zurich) for providing expertise on limited proteolysis and mass spectrometry. Finally, we would like to thank Hayder Shweliyya and his team at the Sahlgrenska University Hospital for fluid biomarker analyses.

Funding

This work was supported by institutional funding of the University of Zurich, a University of Zurich Candoc grant (to C.R.), as well as grants from the Synapsis Foundation—Dementia Research Switzerland (No. 2019-PI06 to R.M.N., C.G., and A.G.), the Swiss National Science Foundation (SNF 33CM30-124111, SNF 320030-125387/1 to C.H.) and the Mäxi Foundation (to C.H.). K.B. is supported by the Swedish Research Council (#2017-00915 and #2022-00732), the Swedish Alzheimer Foundation (#AF-930351, #AF-939721, #AF-968270, and #AF-994551), Hjärnfonden, Sweden (#FO2017-0243 and #ALZ2022-0006), the Swedish state under the agreement between the Swedish government and the County Councils, the ALF-agreement (#ALFGBG-715986 and #ALFGBG-965240), the European Union Joint Program for Neurodegenerative Disorders (JPND2019-466-236), the Alzheimer's Association 2021 Zenith Award (ZEN-21-848495), the Alzheimer's Association 2022-2025 Grant (SG-23-1038904 QC), La Fondation Recherche Alzheimer (FRA), Paris, France, the Kirsten and Freddy Johansen Foundation, Copenhagen, Denmark, and Familjen Rönströms Stiftelse, Stockholm, Sweden. H.Z. is a Wallenberg Scholar and a Distinguished Professor at the Swedish Research Council supported by grants from the Swedish Research Council (#2023-00356; #2022-01018 and #2019-02397), the European Union's Horizon Europe research and innovation programme under grant agreement No 101053962, and Swedish State Support for Clinical Research (#ALFGBG-71320).

Competing interests

T.K. is currently an employee of Charles River Associates, Switzerland; K.B. has served as a consultant and at advisory boards for Abbvie, AC Immune, ALZPath, AriBio, BioArctic, Biogen, Eisai, Lilly, Moleac Pte. Ltd, Neurimmune, Novartis, Ono Pharma, Prothena, Roche Diagnostics, and Siemens Healthineers. He has served at data monitoring committees for Julius Clinical and Novartis. He has given lectures, produced educational materials and participated in educational programs for AC Immune, Biogen, Celdara Medical, Eisai and Roche Diagnostics. He is a co-founder of Brain Biomarker Solutions in Gothenburg AB (BBS), which is a part of the GU Ventures Incubator Program, outside the work presented in this paper; M.T.F is the cofounder of the Women's Brain Project. In the past 2 years, she has received consulting and speaker fees from Roche and Lilly, unrelated to this project. She is currently an employee of Syntropic Medical, Vienna, Austria; L.K. is an employee of Roche, Switzerland; C.H. and R.M.N. are employees and shareholders of Neurimmune AG, Switzerland; Within the past 5 years A.G. has served at advisory boards for Biogen, Eli Lilly, Eisai and participated in clinical trials or research/project collaborations with Biogen, Neurimmune, Schwabe Pharma. He received speaker fees by Eli Lilly and OM-Pharma.

Supplementary material

Supplementary material is available at *Brain* online.

References

1. Gustavsson A, Norton N, Fast T, et al. Global estimates on the number of persons across the Alzheimer's disease continuum. *Alzheimers Dement*. 2023;19:658-670.
2. Jack CR Jr, Bennett DA, Blennow K, et al. NIA-AA research framework: Toward a biological definition of Alzheimer's disease. *Alzheimers Dement*. 2018;14:535-562.
3. Hansson O, Blennow K, Zetterberg H, Dage J. Blood biomarkers for Alzheimer's disease in clinical practice and trials. *Nat Aging*. 2023;3:506-519.
4. van der Kant R, Goldstein LSB, Ossenkoppele R. Amyloid-β-independent regulators of tau pathology in Alzheimer disease. *Nat Rev Neurosci*. 2020;21:21-35.
5. Mattsson-Carlgren N, Salvadó G, Ashton NJ, et al. Prediction of longitudinal cognitive decline in preclinical Alzheimer disease using plasma biomarkers. *JAMA Neurol*. 2023;80:360-369.
6. Sperling RA, Aisen PS, Beckett LA, et al. Toward defining the preclinical stages of Alzheimer's disease: Recommendations from the National Institute on Aging-Alzheimer's Association workgroups on diagnostic guidelines for Alzheimer's disease. *Alzheimers Dement*. 2011;7:280-292.
7. Schindler SE, Li Y, Buckles VD, et al. Predicting symptom onset in sporadic Alzheimer disease with amyloid PET. *Neurology*. 2021;97:e1823-e1834.
8. Donohue MC, Sperling RA, Petersen R, et al. Association between elevated brain amyloid and subsequent cognitive decline among cognitively normal persons. *JAMA*. 2017;317:2305-2316.
9. Ossenkoppele R, Pichet Binette A, Groot C, et al. Amyloid and tau PET-positive cognitively unimpaired individuals are at high risk for future cognitive decline. *Nat Med*. 2022;28:2381-2387.
10. Karikari TK, Pascoal TA, Ashton NJ, et al. Blood phosphorylated tau 181 as a biomarker for Alzheimer's disease: A diagnostic performance and prediction modelling study using data from four prospective cohorts. *Lancet Neurol*. 2020;19:422-433.
11. Dubois B, Villain N, Frisoni GB, et al. Clinical diagnosis of Alzheimer's disease: Recommendations of the International Working Group. *Lancet Neurol*. 2021;20:484-496.
12. Heneka MT, Carson MJ, El Khoury J, et al. Neuroinflammation in Alzheimer's disease. *Lancet Neurol*. 2015;14:388-405.
13. Kunkle BW, Grenier-Boley B, Sims R, et al. Genetic meta-analysis of diagnosed Alzheimer's disease identifies new risk loci and implicates Abeta, tau, immunity and lipid processing. *Nat Genet*. 2019;51:414-430.
14. Gate D, Saligrama N, Leventhal O, et al. Clonally expanded CD8 T cells patrol the cerebrospinal fluid in Alzheimer's disease. *Nature*. 2020;577:399-404.
15. Itagaki S, McGeer PL, Akiyama H. Presence of T-cytotoxic suppressor and leucocyte common antigen positive cells in Alzheimer's disease brain tissue. *Neurosci Lett*. 1988;91:259-264.
16. Togo T, Akiyama H, Iseki E, et al. Occurrence of T cells in the brain of Alzheimer's disease and other neurological diseases. *J Neuroimmunol*. 2002;124:83-92.
17. van Olst L, Kamermans A, Halters S, et al. Adaptive immune changes associate with clinical progression of Alzheimer's disease. *Mol Neurodegener*. 2024;19:38.
18. Gericke C, Kirabali T, Flury R, et al. Early β-amyloid accumulation in the brain is associated with peripheral T cell alterations. *Alzheimers Dement*. 2023;19:5642-5662.
19. Rickenbach C, Gericke C. Specificity of adaptive immune responses in central nervous system health, aging and diseases. *Front Neurosci*. 2022;15:806260.
20. Dhanwani R, Pham J, Premlal ALR, et al. T cell responses to neural autoantigens are similar in Alzheimer's disease patients and age-matched healthy controls. *Front Neurosci*. 2020;14:874.
21. Monsonego A, Zota V, Karni A, et al. Increased T cell reactivity to amyloid beta protein in older humans and patients with Alzheimer disease. *J Clin Invest*. 2003;112:415-422.
22. Zota V, Nemirovsky A, Baron R, et al. HLA-DR alleles in amyloid beta-peptide autoimmunity: A highly immunogenic role for the DRB1*1501 allele. *J Immunol*. 2009;183:3522-3530.
23. Schenk C, Barbour R, Dunn W, et al. Immunization with amyloid-β attenuates Alzheimer-disease-like pathology in the PDAPP mouse. *Nature*. 1999;400:173-177.
24. Nicoll JA, Wilkinson D, Holmes C, Steart P, Markham H, Weller RO. Neuropathology of human Alzheimer disease after immunization with amyloid-beta peptide: A case report. *Nat Med*. 2003;9:448-452.
25. Lee M, Bard F, Johnson-Wood K, et al. Aβ42 immunization in Alzheimer's disease generates Aβ N-terminal antibodies. *Ann Neurol*. 2005;58:430-435.
26. Gaskin F, Finley J, Fang Q, Xu S, Fu SM. Human antibodies reactive with beta-amyloid protein in Alzheimer's disease. *J Exp Med*. 1993;177:1181-1186.
27. Maftei M, Thurm F, Schnack C, et al. Increased levels of antigen-bound beta-amyloid autoantibodies in serum and cerebrospinal fluid of Alzheimer's disease patients. *PLoS One*. 2013;8:e68996.
28. Sevigny J, Chiao P, Bussière T, et al. The antibody aducanumab reduces Aβ plaques in Alzheimer's disease. *Nature*. 2016;537:50-56.
29. Winblad B, Palmer K, Kivipelto M, et al. Mild cognitive impairment—Beyond controversies, towards a consensus: Report of the International Working Group on Mild Cognitive Impairment. *J Intern Med*. 2004;256:240-246.
30. Bachmann D, Buchmann A, Studer S, et al. Age-, sex-, and pathology-related variability in brain structure and cognition. *Transl Psychiatry*. 2023;13:278.
31. Klunk WE, Koeppe RA, Price JC, et al. The centiloid project: Standardizing quantitative amyloid plaque estimation by PET. *Alzheimers Dement*. 2015;11:1-15.e154.
32. Salvadó G, Molinuevo JL, Brugulat-Serrat A, et al. Centiloid cut-off values for optimal agreement between PET and CSF core AD biomarkers. *Alzheimers Res Ther*. 2019;11:27.
33. World Medical Association. World Medical Association Declaration of Helsinki: Ethical principles for medical research involving human subjects. *JAMA*. 2013;310:2191-2194.
34. Hixson JE, Vernier DT. Restriction isotyping of human apolipoprotein E by gene amplification and cleavage with HhaI. *J Lipid Res*. 1990;31:545-548.
35. Bachmann D, Roman ZJ, Buchmann A, et al. Lifestyle affects amyloid burden and cognition differently in men and women. *Ann Neurol*. 2022;92:451-463.
36. Antweiler RC, Taylor HE. Evaluation of statistical treatments of left-censored environmental data using coincident uncensored data sets: I. Summary statistics. *Environ Sci Technol*. 2008;42:3732-3738.
37. Kassambara A. rstatix: pipe-friendly framework for basic statistical tests [R package]. Version 0.7.2. Comprehensive R Archive Network (CRAN); 2023. doi: 10.32614/CRAN.package.rstatix
38. Kivisäkk P, Tucky B, Wei T, Campbell JJ, Ransohoff RM. Human cerebrospinal fluid contains CD4+ memory T cells expressing gut- or skin-specific trafficking determinants: Relevance for immunotherapy. *BMC Immunol*. 2006;7:14.
39. Wozniak MA, Mee AP, Itzhaki RF. Herpes simplex virus type 1 DNA is located within Alzheimer's disease amyloid plaques. *J Pathol*. 2009;217:131-138.
40. Warren-Gash C, Forbes HJ, Williamson E, et al. Human herpesvirus infections and dementia or mild cognitive impairment: A systematic review and meta-analysis. *Sci Rep*. 2019;9:4743.

41. Feng Y, De Franceschi G, Kahraman A, et al. Global analysis of protein structural changes in complex proteomes. *Nat Biotechnol*. 2014;32:1036-1044.
42. Buchholz S, Zempel H. The six brain-specific TAU isoforms and their role in Alzheimer's disease and related neurodegenerative dementia syndromes. *Alzheimers Dement*. 2024;20:3606-3628.
43. Jensen KK, Andreatta M, Marcatili P, et al. Improved methods for predicting peptide binding affinity to MHC class II molecules. *Immunology*. 2018;154:394-406.
44. Nilsson JB, Kaabinejadian S, Yari H, et al. Accurate prediction of HLA class II antigen presentation across all loci using tailored data acquisition and refined machine learning. *Sci Adv*. 2023;9: eadj6367.
45. Lindestam Arlehamn CS, Pham J, Alcalay RN, et al. Widespread tau-specific CD4 T cell reactivity in the general population. *J Immunol*. 2019;203:84-92.
46. Campisi L, Chizari S, Ho JSY, et al. Clonally expanded CD8 T cells characterize amyotrophic lateral sclerosis-4. *Nature*. 2022;606: 945-952.
47. Jorfi M, Park J, Hall CK, et al. Infiltrating CD8(+) T cells exacerbate Alzheimer's disease pathology in a 3D human neuroimmune axis model. *Nat Neurosci*. 2023;26:1489-1504.
48. GIannakopoulos P, Herrmann FR, Bussière T, et al. Tangle and neuron numbers, but not amyloid load, predict cognitive status in Alzheimer's disease. *Neurology*. 2003;60:1495-1500.
49. Yu L, Boyle PA, Janelidze S, et al. Plasma p-tau181 and p-tau217 in discriminating PART, AD and other key neuropathologies in older adults. *Acta Neuropathol*. 2023;146:1-11.
50. Chen X, Firulyova M, Manis M, et al. Microglia-mediated T cell infiltration drives neurodegeneration in tauopathy. *Nature*. 2023;615:668-677.
51. Merlini M, Kirabali T, Kulic L, Nitsch RM, Ferretti MT. Extravascular CD3+ T cells in brains of Alzheimer disease patients correlate with tau but not with amyloid pathology: An immunohistochemical study. *Neurodegener Dis*. 2018;18:49-56.
52. Horie K, Salvadó G, Barthélemy NR, et al. CSF MTBR-tau243 is a specific biomarker of tau tangle pathology in Alzheimer's disease. *Nat Med*. 2023;29:1954-1963.
53. Su W, Saravia J, Risch I, et al. CXCR6 orchestrates brain CD8(+) T cell residency and limits mouse Alzheimer's disease pathology. *Nat Immunol*. 2023;24:1735-1747.
54. Lindestam Arlehamn CS, Garretti F, Sulzer D, Sette A. Roles for the adaptive immune system in Parkinson's and Alzheimer's diseases. *Curr Opin Immunol*. 2019;59:115-120.
55. Lee H, Jeong S, Shin EC. Significance of bystander T cell activation in microbial infection. *Nat Immunol*. 2022;23:13-22.
56. Luo G, Ambati A, Lin L, et al. Autoimmunity to hypocretin and molecular mimicry to flu in type 1 narcolepsy. *Proc Natl Acad Sci U S A*. 2018;115:E12323-E12332.
57. Sospedra M, Martin R. Immunology of multiple sclerosis. *Annu Rev Immunol*. 2005;23:683-747.
58. Wang J, Jelcic I, Mühlenbruch L, et al. HLA-DR15 molecules jointly shape an autoreactive T cell repertoire in multiple sclerosis. *Cell*. 2020;183:1264-1281.e20.
59. Zheng H, Koo EH. Biology and pathophysiology of the amyloid precursor protein. *Mol Neurodegener*. 2011;6:27.
60. Gremer L, Schölzel D, Schenk C, et al. Fibril structure of amyloid-β(1–42) by cryo–electron microscopy. *Science*. 2017;358: 116-119.
61. Iadanza MG, Jackson MP, Hewitt EW, Ranson NA, Radford SE. A new era for understanding amyloid structures and disease. *Nat Rev Mol Cell Biol*. 2018;19:755-773.
62. Evin G, Zhu A, Holsinger RM, Masters CL, Li QX. Proteolytic processing of the Alzheimer's disease amyloid precursor protein in brain and platelets. *J Neurosci Res*. 2003;74:386-392.
63. Baruch K, Rosenzweig N, Kertser A, et al. Breaking immune tolerance by targeting Foxp3(+) regulatory T cells mitigates Alzheimer's disease pathology. *Nat Commun*. 2015;6:7967.
64. Rosenzweig N, Dvir-Szternfeld R, Tsitsou-Kampeli A, et al. PD-1/PD-L1 checkpoint blockade harnesses monocyte-derived macrophages to combat cognitive impairment in a tauopathy mouse model. *Nat Commun*. 2019;10:465.
65. Ben-Yehuda H, Arad M, Peralta Ramos JM, et al. Key role of the CCR2-CCL2 axis in disease modification in a mouse model of tauopathy. *Mol Neurodegener*. 2021;16:39.
66. Marin-Rodero M, Cintado E, Walker AJ, et al. The meninges host a distinct compartment of regulatory T cells that preserves brain homeostasis. *Sci Immunol*. 2025;10:eadu2910.
67. Alves S, Churlaud G, Audrain M, et al. Interleukin-2 improves amyloid pathology, synaptic failure and memory in Alzheimer's disease mice. *Brain*. 2017;140:826-842.
68. Dansokho C, Ait Ahmed D, Aid S, et al. Regulatory T cells delay disease progression in Alzheimer-like pathology. *Brain*. 2016; 139(Pt 4):1237-1251.
69. Faridar A, Vasquez M, Thome AD, et al. Ex vivo expanded human regulatory T cells modify neuroinflammation in a preclinical model of Alzheimer's disease. *Acta Neuropathol Commun*. 2022;10:144.
70. Harris F, Berdugo YA, Tree T. IL-2-based approaches to Treg enhancement. *Clin Exp Immunol*. 2023;211:149-163.
71. Aisen PS, Davis KL, Berg JD, et al. A randomized controlled trial of prednisone in Alzheimer's disease. Alzheimer's disease cooperative study. *Neurology*. 2000;54:588-593.
72. Ferretti MT, Merlini M, Späni C, et al. T-cell brain infiltration and immature antigen-presenting cells in transgenic models of Alzheimer's disease-like cerebral amyloidosis. *Brain Behav Immun*. 2016;54:211-225.
73. Gericke C, Mallone A, Engelhardt B, Nitsch RM, Ferretti MT. Oligomeric forms of human amyloid-Beta(1-42) inhibit antigen presentation. *Front Immunol*. 2020;11:1029.
74. Aversa G, Punnonen J, Cocks BG, et al. An interleukin 4 (IL-4) mutant protein inhibits both IL-4 or IL-13-induced human immunoglobulin G4 (IgG4) and IgE synthesis and B cell proliferation: Support for a common component shared by II,-4 and IL-13 receptors. *J Exp Med*. 1993;178:2213-2218.
75. Tuzlak S, Dejean AS, Iannacone M, et al. Repositioning T(H) cell polarization from single cytokines to complex help. *Nat Immunol*. 2021;22:1210-1217.
76. Bernstein ZJ, Shenoy A, Chen A, Heller NM, Spangler JB. Engineering the IL-4/IL-13 axis for targeted immune modulation. *Immunol Rev*. 2023;320:29-57.
77. Wang J, Gu BJ, Masters CL, Wang YJ. A systemic view of Alzheimer disease—Insights from amyloid-β metabolism beyond the brain. *Nat Rev Neurol*. 2017;13:612-623.
78. Gu BJ, Huang X, Ou A, et al. Innate phagocytosis by peripheral blood monocytes is altered in Alzheimer's disease. *Acta Neuropathol*. 2016;132:377-389.
79. Altendorfer B, Unger MS, Poupardin R, et al. Transcriptomic profiling identifies CD8(+) T cells in the brain of aged and Alzheimer's disease transgenic mice as tissue-resident memory T cells. *J Immunol*. 2022;209:1272-1285.
80. Arndt JW, Qian F, Smith BA, et al. Structural and kinetic basis for the selectivity of aducanumab for aggregated forms of amyloid-β. *Sci Rep*. 2018;8:6412.
81. Chen Y, Wei G, Zhao J, Nussinov R, Ma B. Computational investigation of gantenerumab and crenezumab recognition of Aβ fibrils in Alzheimer's disease brain tissue. *ACS Chem Neurosci*. 2020;11:3233-3244.
82. Geylis V, Kourilov V, Meiner Z, Nennesmo I, Bogdanovic N, Steinitz M. Human monoclonal antibodies against amyloid-beta from healthy adults. *Neurobiol Aging*. 2005;26:597-606.